Available online at www.sciencedirect.com

SciVerse ScienceDirect

Ceramics International 38 (2012) 3175–3183

CERAMICS INTERNATIONAL

www.elsevier.com/locate/ceramint

Low temperature cofirable $Ca[(Li_{1/3}Nb_{2/3})_{0.95}Zr_{0.15}]O_{3+\delta}$ microwave dielectric ceramic with $ZnO–B_2O_3–SiO_2$ frit

Mingzhe Hu [a,b,*], Juan Xiong [b], Haoshuang Gu [b], Yihang Chen [a], Yu Wang [a]

[a] Department of Applied Physics and Materials Research Center, The Hong Kong Polytechnic University, Hong Kong Special Administrative Region

[b] Faculty of Electronic Science & Technology, Hubei University, Xueyuan Road, Wuhan 430062, China

Received 3 August 2011; received in revised form 13 December 2011; accepted 13 December 2011
Available online 22 December 2011

Abstract

The sintering properties and microwave dielectric properties of $Ca[(Li_{1/3}Nb_{2/3})_{1-x}Zr_{3x}]O_{3+\delta}$ ($x = 0.05$, abbreviated as CLNZ) ceramic doped with ZBS frit are investigated for LTCC applications. XRD patterns and SEM photographs show that dense and single perovskite phase ceramics can be obtained with ZBS doping content of less than 10 wt%, before the $Ca_2Nb_2O_7$ pyrochlore phase begins to segregates. The results show that ZBS vitreous phase stays at the grain boundary in the final sintered ceramics, suggesting it acts as liquid phase lubrication during sintering, and has effectively lowered the sintering temperature of CLNZ ceramics from 1170 °C to 940 °C. The preferred orientation of CLNZ solid solution varies from (1 2 1) plane to (1 0 1) plane as ZBS content and sintering temperature increase. The optimal microwave dielectric properties of $\varepsilon_r = 32.0$, $Q_f = 6.64$ THz and $\tau_f = -27.1$ ppm/°C can be obtained in 15 wt% ZBS doped CLNZ ceramic when sintered at 940 °C for 4 h. The Ag-cofiring experiment clearly shows that no chemical reaction takes place between Ag and the ZBS-doped CLNZ ceramic, indicating its great potential applications in LTCC field.

Keywords: ZBS frit; Microwave dielectric properties; Low temperature cofire sintering; Addition

1. Introduction

Since ultrahigh frequency multilayered circuit is effective in miniaturizing various kinds of microwave modules and substrates, it has become one of the most exciting areas in microwave communication devices over the past decade [1–4]. In order to develop such highly packaged microwave circuits, ceramics are required to be cofired with interlayered metals such as Cu, Au and Ag with lower sintering temperatures than that of the metal melting point (1080 °C for Cu, 1060 °C for Au and 960 °C for Ag), which is known as low temperature cofired ceramics (LTCC) technology. Recently, a number of studies have been conducted to develop LTCC materials and among these materials, $Ca(Li_{1/3}Nb_{2/3})O_{3-\delta}$-based complex perovskite ceramic, which was first reported by Choi et al. [5], is an excellent candidate. This material possesses an outstanding quality factor value of 40 THz with a medium dielectric constant of 29.6 at room temperature. However, the large negative temperature coefficient of resonant frequency (τ_f value) would require further adjustment for practical applications. According to Choi et al., when $(Li_{1/3}Nb_{2/3})^{3.67+}$ complex ions were substituted by 20 mol% Ti^{4+} ions at B-site, the τ_f value could be stabilized to nearly zero. In our previous research, we also found that Zr^{4+} nonstoichiometric substitution for B-site $(Li_{1/3}Nb_{2/3})^{3.67+}$ could effectively modify the large negative τ_f value of $Ca(Li_{1/3}Nb_{2/3})O_{3-\delta}$ ceramic. Moreover, since Li^+ is an evaporable element during ceramic sintering, which will result in oxygen vacancies and deteriorate the Q_f value of $Ca(Li_{1/3}Nb_{2/3})O_{3-\delta}$ ceramic, Zr^{4+} nonstoichiometric substitution for B-site $(Li_{1/3}Nb_{2/3})^{3.67+}$ could compensate for these oxygen vacancies and improve the Q_f value. However, the sintering temperature for these $Ca(Li_{1/3}Nb_{2/3})O_{3-\delta}$-based ceramics (above 1150 °C) is too high to be cofired with Ag. The addition of low melting point oxides or glasses has been a common way to lower the sintering temperature of

* Corresponding author at: Faculty of Electronic Science & Technology, Hubei University, Wuhan.
E-mail address: mzhu74@hubu.edu.cn (M. Hu).

0272-8842/$36.00
doi:10.1016/j.ceramint.2011.12.021

microwave dielectric ceramics in both academic and industrial circles because of its efficiency and low cost [6–8] and a number of investigations have focused on using single phase oxide to lower the sintering temperature of $Ca(Li_{1/3}Nb_{2/3})O_{3-\delta}$-based ceramics. For examples, 4 wt% Bi_2O_3 doping could effectively lower the sintering temperature of $Ca[(Li_{1/3}Nb_{2/3})_{0.8}Ti_{0.2}]O_{3-\delta}$ ceramic to 1050 °C with good microwave dielectric properties of $\varepsilon_r = 37.8$, $Q_f = 11030$ GHz and $\tau_f = 12$ ppm/°C [9], while 0.7 wt% B_2O_3 doping could lower the sintering temperature of $Ca[(Li_{1/3}Nb_{2/3})_{0.9}Ti_{0.1}]O_{3-\delta}$ ceramic to 1000 °C and produce excellent microwave properties of $\varepsilon_r = 35$, $Q_f = 21000$ GHz and $\tau_f = -5.6$ ppm/°C [10]. However, from the viewpoint of eutectic solution, multicomponent doping, such as $B_2O_3 + SiO_2$ borosilicate glass, can form a more stable compound with lower melting point than a single phase doping system, such as B_2O_3 doping, so multicomponent glass can lower the sintering temperature more efficiently. Different kinds of borosilicate glasses have been developed for LTCC applications [11–13], such as $BaO–B_2O_3–SiO_2$, $CaO–B_2O_3–SiO_2$, $ZnO–B_2O_3–SiO_2$, $Li_2O–B_2O_3–SiO_2$ and so on. Among them, $60ZnO–30B_2O_3–10SiO_2$ (ZBS) glass has a low melting point of ~560 °C with low dielectric loss at microwave frequency. Therefore, it is expected that ZBS doped $Ca[(Li_{1/3}Nb_{2/3})_{1-x}Zr_{3x}]O_{3+\delta}$ ($x = 0.05$, abbreviated as CLNZ hereafter) ceramic might have great potential for LTCC technology application. In the present article, the sintering behavior, phase assemblage and the microwave dielectric properties of ZBS doped CLNZ ceramics are examined. The liquid phase sintering mechanism of ZBS glass will be discussed with results illustrating that ZBS glass is effective for lowering the sintering temperature of CLNZ ceramic.

2. Experimental procedures

2.1. Sample preparation

High purity (>99%) raw materials $CaCO_3$, Li_2CO_3, Nb_2O_5 and ZrO_2 were weighed according to the desired stoichiometry. The batched powders were mixed with ethanol medium and planetary milled for 4 h. The slurry was pan dried and calcined at 900 °C for 2 h. ZBS glass was made by batching desired weight percentage of ZnO (60 wt%), B_2O_3 (30 wt%) and SiO_2 (10 wt%) powders. The batched powder was mixed by planetary milling for 4 h before it was pan-dried and heated up to its melting point. Then the melting glass was quenched in air and powdered for addition. The calcined CLNZ powder was weighed with desired content of ZBS glass powder and milled for another 4 h, pan dried and granulated with 5 wt% PVA. The mixed powders were then pelleted into 7–8 mm high cylinders with 15 mm diameter under a uniaxial pressure of 150 MPa. The final sintering process was carried out at 940–1060 °C for 4 h in closed Al_2O_3 crucibles. The pellets were sintered under the support of calcined powder with the same chemical composition to prevent the evaporation of Li^+. For coating with Ag electrode process, the samples were screen printed with high purity Ag slurry (Ag content > 80 wt%) and annealed at 500 °C for 20 min.

2.2. Sample characterization

The apparent density of the sample was directly measured by the ratio of weight and volume. The theoretical density of CLNZ ceramic was calculated using the XRD data and the theoretical density of ZBS glass was measured by Archimedes method. The phase assemblage was detected by X-ray method (Bruker D8 Discover) using CuKα radiation. The microstructure properties were observed under a scanning electron microscope (SEM) (JEOL 6490). The glass transition temperature was examined through differential thermal and thermogravimetric (DTA–TG) analysis ranging room temperature to 1100 °C in air with a thermal analyzer Netzsch STA449C, Jupiter Equipment. The thermal expansion coefficient and the thermal conductivity of the sample with the optimal microwave dielectric properties were tested by using instruments Netzsch DIL402C and Decagon KD2 Pro respectively. Microwave dielectric properties were measured by Hakki-Coleman open resonator method using Agilent 8720ES vector network analyzer. TE_{011} modes, resonating in 4–7 GHz frequency range, were employed for the measurement. The temperature coefficient was measured by a digital controllable thermalstat in the temperature range of 20–80 °C.

3. Results and discussion

3.1. Sintering behavior

Fig. 1 presents the DTA properties of ZBS glass and 10 wt% ZBS glass doped CLNZ ceramic. As can be seen, the first exothermic peak, or the melting point, of ZBS glass locates at around 520 °C. However, it shifts down to about 470 °C for 10 wt% ZBS doped CLNZ ceramic, suggesting that the liquid phase generation temperature has lowered by ~50 °C. Such drop might be a result of alkali ion (Li^+) acting as a modifier, in which it breaks into the chemical bonds in the ZBS glass network at low temperature and helps to further reduce the melting point of ZBS glass, benefiting the grain-to-grain mass transfer in liquid phase sintering [14].

Fig. 2(a) shows how the relative density of CLNZ + x wt% ZBS-doped ceramics varies with sintering temperatures and chemical compositions. The relative densities of various ZBS content doped CLNZ samples were calculated by using the apparent densities divided by theirs corresponding theoretical

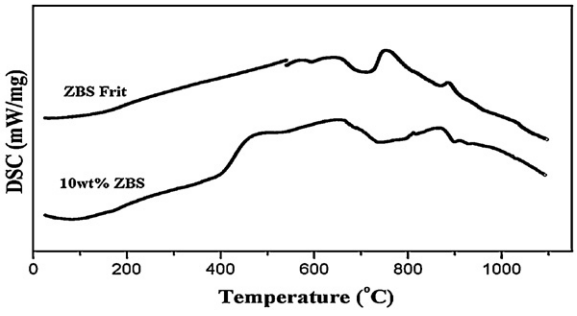

Fig. 1. DSC curve of CLNZ ceramic and 10 wt% ZBS doped CLNZ ceramic.

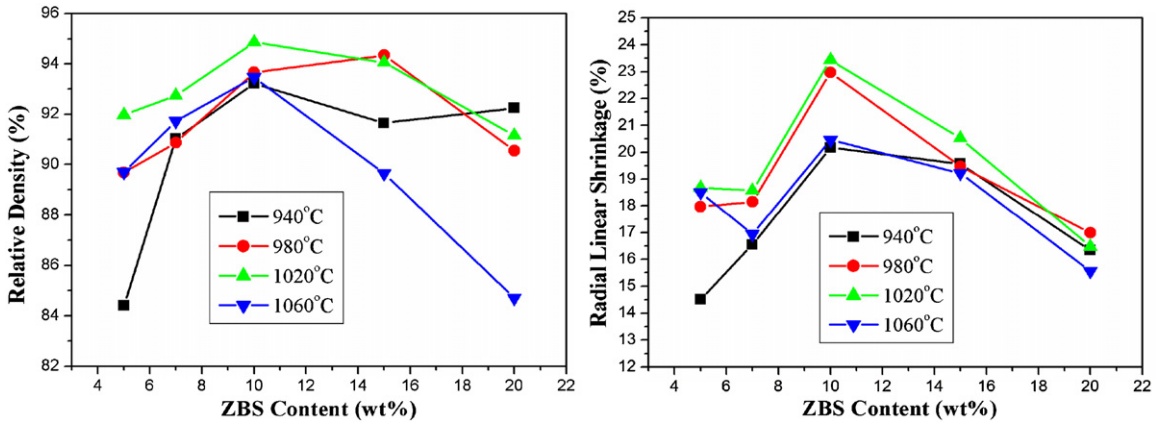

Fig. 2. Relative density and radial linear shrinkage of CLNZ ceramics varied with ZBS contents and sintering temperatures.

densities with the following formula [15]:

$$\rho = \frac{W_1 + W_2}{W_1/\rho_1 + W_2/\rho_2} \quad (1)$$

where W_1, W_2 are the weight of CLNZ ceramic and ZBS glass while ρ_1 and ρ_2 are the theoretical density of CLNZ ceramic (4.48 g/cm^3) and ZBS glass (4.87 g/cm^3) respectively. As can be seen from the figure, the relative density first increases with increasing ZBS content until it reaches the maximum value of $x = 10$ before it drops gradually with further increase of ZBS content. The linear shrinkage of the above ceramics varies similarly with the relative density as illustrated in Fig. 2(b). Generally, more ZBS doping content will generate more liquid phase during sintering process, which is beneficial for ceramic densification. However, when ZBS doping content exceeds 10 wt%, pores and vacancies are formed easily due to the evaporation of ZBS glass during sintering, which is suggested to be responsible for the decreased relative density and linear shrinkage after $x = 10$. Moreover, the densification temperature decreases with increasing x value. For $x \leq 10$, the maximum densities are obtained at 1020 °C, while for $x = 15$ and 20, the maximum density is obtained at 980 °C and 940 °C respectively. The highest relative density of 94.86% as well as the maximum radial linear shrinkage of 23.43% are simultaneously obtained in 10 wt% ZBS doped sample when sintered at 1020 °C. Very poor relative density of less than 85% can be found in both small ZBS content (5 wt%) doped sample sintered at 940 °C and in high ZBS content (20 wt%) doped sample sintered at 1060 °C. The former might be a result of insufficient grain growth of CLNZ ceramic, while the latter is due to the evaporation of ZBS glass as well as the rapid growth of CLNZ grains, which results in a large amount of closed pores in the final ceramic [16]. When taking into account that the pure CLNZ ceramic is densified at 1170 °C with a relative density of 94.28%, one may conclude that ZBS is an effective sintering aid for CLNZ ceramic.

3.2. Phase formation and microstructure

Fig. 3 shows how the XRD patterns of CLNZ ceramic vary with x wt% ZBS ($x = 5$, 7, 10, 15, and 20) glass additions and sintering temperatures. As can be seen, the CLNZ ceramic exhibits a distorted perovskite structure with orthorhombic *Pbmn* space group; however, the crystal orientation of the CLNZ ceramic varies with chemical composition in 1020 °C sintered specimens, as illustrated in Fig. 3(a) and (b). The intensity ratio of (1 0 1) to (1 2 1) crystal plane has an almost linear dependence on ZBS glass content, suggesting an anisotropic grain growth of CLNZ ceramic. This phenomenon has also been observed by several other authors [17–19] and we believe this could be attributed to the anisotropic interface diffusion rate in CLNZ orthorhombic structure. Originally, the interface diffusion energy of (1 0 1) crystal plane is higher than that of the (1 2 1) crystal plane, thus, the latter has a faster interface migration velocity. However, under the inducement of ZBS viscous phase, the interface diffusion energy of (1 0 1) crystal plane is gradually reduced and becomes energetically superior to the (1 2 1) crystal plane, resulting in the final (1 0 1) preferred orientation. Single perovskite phase ceramic can be produced until ZBS glass content reaches 10 wt% before a small amount of $Ca_2Nb_2O_7$-type second phase can be detected and its content increases with the increase of ZBS glass, suggesting extensive chemical reactions might have taken place between CLNZ ceramic and ZBS glass during sintering. Also, the impurity phase varies with the sintering temperature for the same chemical composition. For example, in 15 wt% ZBS doped sample, about 28%, 24% and 20% volume percentage $Ca_2Nb_2O_7$-type second phase were found in 940 °C, 980 °C and 1060 °C sintered samples respectively. However, we suggest that the chemical composition is different in these $Ca_2Nb_2O_7$-type phases because the preferential crystal planes of these impurity phases are different, as illustrated in Fig. 3(e).

Fig. 4 presents SEM pictures of CLNZ + x wt% ZBS ceramics sintered at 1020 °C for 4 h. It can be seen that the average grain size gradually increases as x values increases and it saturates after $x = 15$. The grains exhibit approximate equiaxial morphology in $x < 15$ samples, yet the grains begin to feature an elongated morphology when $x \geq 15$, which corresponds very well with the XRD patterns, indicating a preferred (1 0 1) orientation in $x \geq 15$ samples. A vitreous phase can be clearly found at grain boundary in $x \geq 7$ samples,

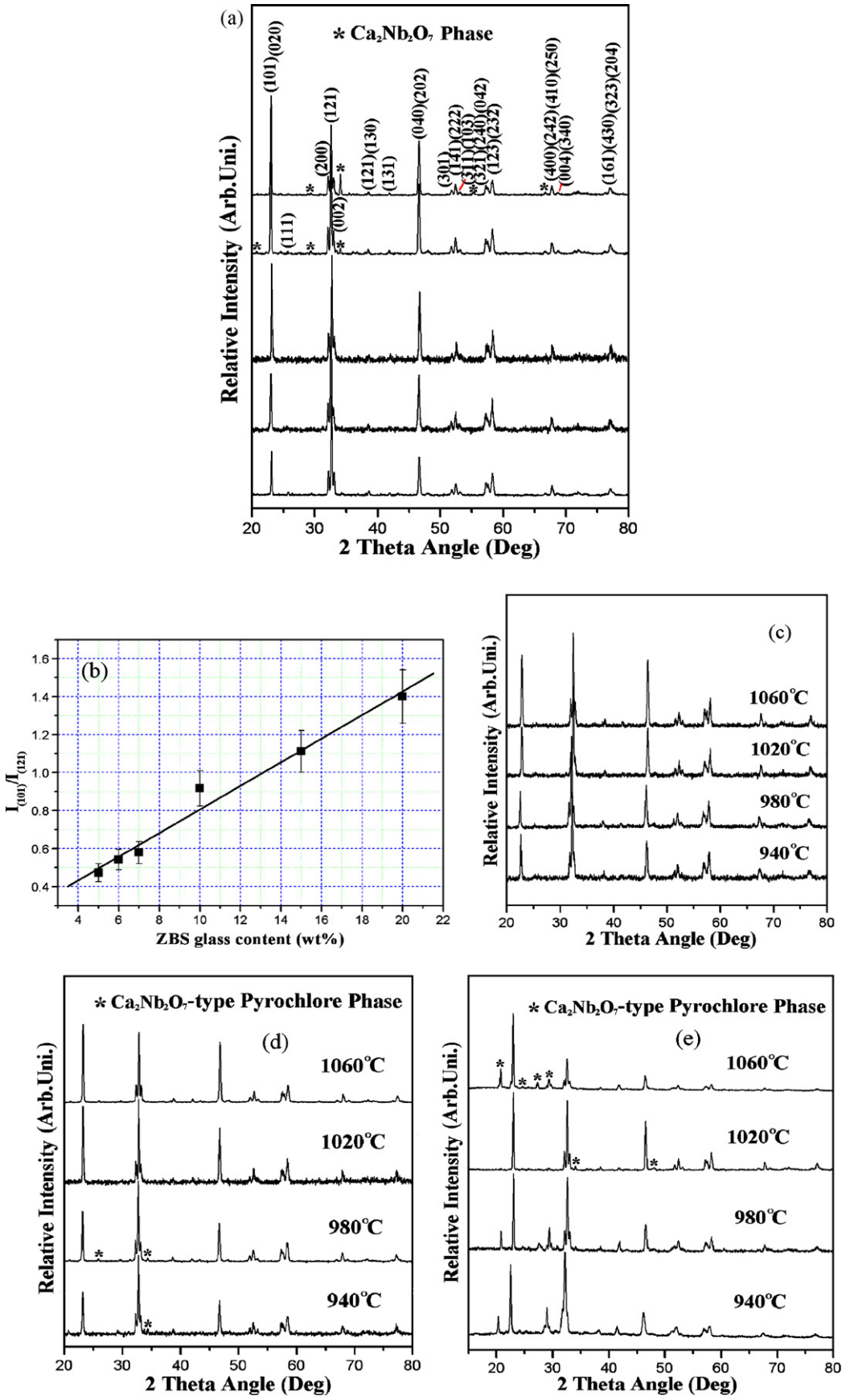

Fig. 3. (a) XRD patterns of $Ca[(Li_{1/3}Nb_{2/3})_{0.95}Zr_{0.15}]O_{3+\delta}$ + x wt% ZBS (x = 5, 7, 10, 15, 20) ceramics sintered at 1020 °C for 4 h. (b) The ratio of (1 0 1) and (1 2 1) peak intensity varied with x value. (c)–(e) XRD patterns of x = 7, 10 and 15 ZBS doped ceramics sintered at different temperatures for 4 h.

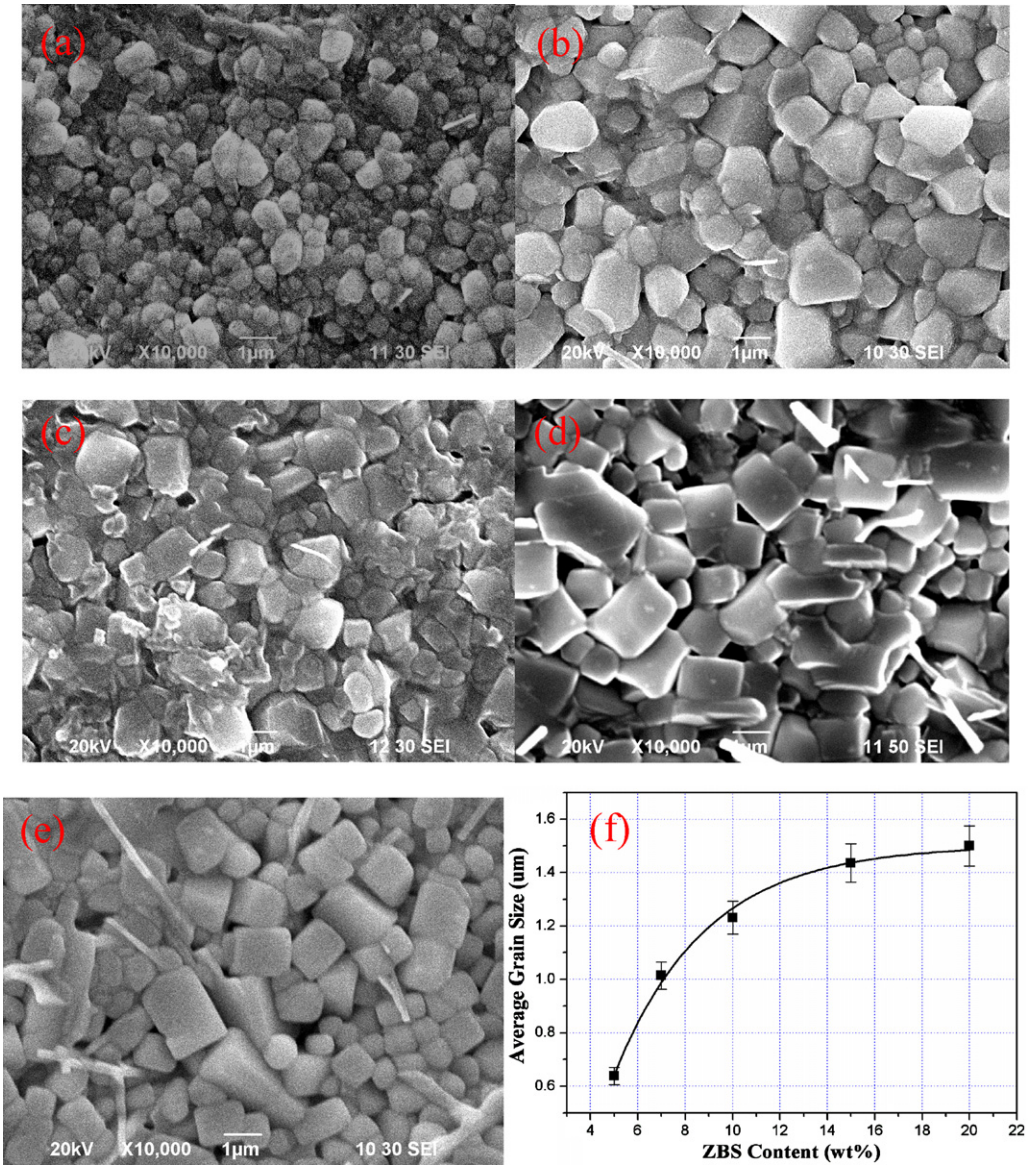

Fig. 4. SEM photographs of $Ca[(Li_{1/3}Nb_{2/3})_{0.95}Zr_{0.15}]O_{3+\delta}$ + x wt% ZBS ceramics sintered at 1020 °C for 4 h. x = (a) 5 wt%, (b) 7 wt%, (c) 10 wt%, (d) 15 wt%, (e) 20 wt%, and (f) average grain size established from SEM photographs.

implying the grain growth is controlled by liquid phase sintering process in ZBS doped CLNZ ceramics. Thus, the densification temperature can be lowered because of the fast grain-to-grain mass transfer speed in liquid phase sintering. However, when a large amount of liquid phase is generated (in $x \geq 15$ samples), the densification is degraded because of the evaporation of ZBS glass [20]. Some rod-like secondary phases can also be observed in $x > 7$ samples and it should be the $Ca_2Nb_2O_7$-type pyrochlore phase according to the XRD analysis in Fig. 3.

3.3. Microwave dielectric properties

Fig. 5 illustrates how ε_r varies with chemical compositions and sintering temperatures in CLNZ + x wt% ZBS ceramics. It is known that dielectric constant relates closely to relative

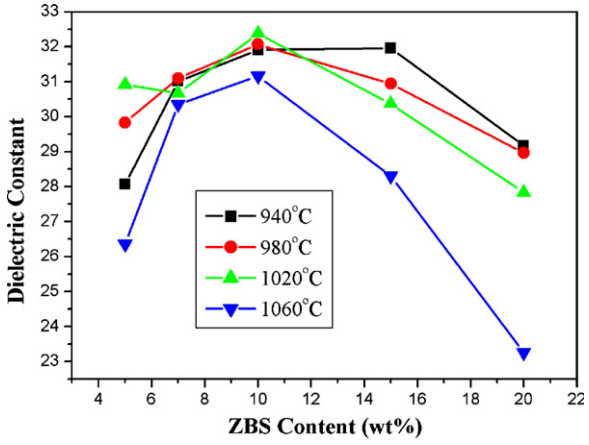

Fig. 5. ε_r varied with chemical compositions and sintering temperatures in CLNZ + x wt% ZBS ceramics.

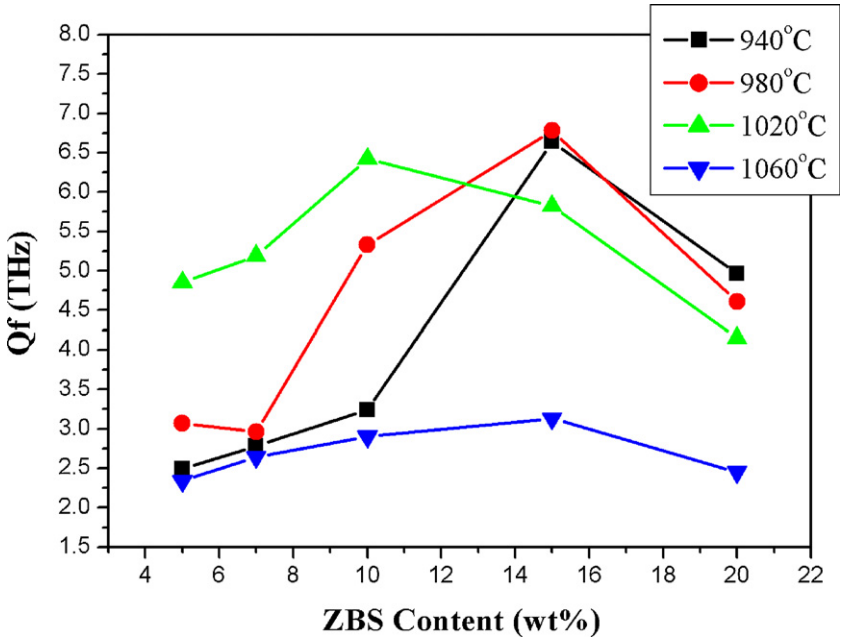

Fig. 6. Q_f value of CLNZ + x wt% ZBS ceramics varied with chemical compositions and sintering temperatures.

density, cell volume, polarizability and secondary phase in ceramics [21–23]. In this case, the variation trend of ε_r is quite similar to that of relative density (please refer to Fig. 2). It firstly increases as x value increases until it reaches the maximum value of $x = 10$ before decreasing with further increase of ZBS content. In the range of $x \leq 10$, the optimal ε_r value is obtained at the sintering temperature of 1020 °C, which can be also ascribed to the relative density effect. The maximum ε_r value of 32.4 is obtained at $x = 10$ when sintered at 1020 °C due to its highest relative density. However, in the range of $x > 10$, this trend seems broken as ε_r has become inconsistent with the variation of relative density and decreases with increasing sintering temperature. Note that $Ca_2Nb_2O_7$-type pyrochlore phase appears in this range and its content increases when sintering temperature deviates from 1020 °C (please refer to Fig. 3(b)). It has been reported that $Ca_2Nb_2O_7$ pyrochlore phase has a dielectric constant of ~27.0 at 1 MHz [24], similar to that of CLNZ perovskite main phase. However, Li^+, as well as the ions from ZBS frit, might also incorporate into the $Ca_2Nb_2O_7$ crystal lattice, which can be indicated by the different crystal orientations of $Ca_2Nb_2O_7$ phase in Fig. 3(e), and this might change the dielectric constant of $Ca_2Nb_2O_7$ phase. Since this chemical composition effect outweighs the relative density effect, the maximum ε_r value is not obtained at the highest relative density point in $x > 10$ samples. For example, in the $x = 15$ sample, the maximum ε_r value of 32.0 is obtained when sintered at 940 °C, instead of at 980 °C, where the highest relative density is obtained. Taking into account that the dielectric constant of pure CLNZ ceramic is 31.6 when sintered at 1170 °C for 4 h with a relative density of 94.3%, one may conclude that ZBS glass addition has lowered the sintering temperature of CLNZ ceramic by 230 °C as well as increased its ε_r value.

The variation of Q_f value with chemical composition and sintering temperature in CLNZ + x wt% ZBS ceramics is shown in Fig. 6. As can be seen, the Q_f value first increases with increasing ZBS content until it reaches the maximum value at $x = 15$ (except for samples sintered at 1020 °C when the maximum value is obtained at $x = 10$) before it decreases with further ZBS frit doping. The highest Q_f value of 6.8 THz can be obtained at $x = 15$ when sintered at 980 °C. The variation trend of Q_f value is similar to that of relative density, but the maximum value is not synchronously obtained. It is quite common that in glass-doped microwave ceramics, Q_f value can only be improved in a limited glass doping content due to the enhancement of relative density as well as the elimination of oxygen vacancies [25,26] yet when a large amount of glass is incorporated, the formation of impurity phase will become a detrimental factor to Q_f value. The impurity phase usually stems from two channels: continuous excess inactive glass phase distributed around grain boundary and the reaction between the vitreous phase and ceramic. In the first case, since ions are weakly bonded in a glassy network in amorphous materials [27], which dissipates and absorbs microwave energy heavily, the Q_f value is substantially reduced in ZBS doped CLNZ ceramics when compared with the Q_f value of 15.0 THz in pure CLNZ ceramic. However, in the second case, it seems that the $Ca_2Nb_2O_7$-type pyrochlore phase has not worsened the Q_f value in ZBS doped CLNZ ceramics. For example, according to the calculation of XRD pattern, about 28% volume percentage $Ca_2Nb_2O_7$-type pyrochlore phase can be found in the $x = 15$ sample when sintered at 940 °C, much higher than that (about 8% volume percentage) in the $x = 10$ sample when sintered at 1020 °C. However, the Q_f value of the former is still larger than the latter despite the fact that the latter possesses both a higher relative density and less vitreous phase content than the

former. This clearly shows that the $Ca_2Nb_2O_7$-type pyrochlore phase in the present system possesses a high Q_f value in microwave frequency, which would be worthwhile for further investigation in the future.

Fig. 7 shows how the temperature coefficient of resonant frequency τ_f varies with chemical compositions and sintering temperatures in CLNZ + x wt% ZBS ceramics sintered at 1020 °C. It can be seen that the τ_f value becomes more negative from −19.6 ppm/°C to −43.2 ppm/°C with increasing ZBS glass content, especially in the range of $x \geq 7$ when the τ_f value decreases much faster, as shown in Fig. 7(a). This reveals that ZBS glass possesses a large negative τ_f value, which is consistent with the investigation of Joseph et al. [28]. The loosely connected ions in vitreous materials, which vibrate in a larger room due to volume expansion as temperature increases, result in an increased dielectric constant, or an increased positive temperature coefficient of dielectric constant, τ_ε. Because τ_ε is related to τ_f as: $\tau_f = -(1/2)\tau_\varepsilon - \alpha_L$, where α_L is the linear thermal-expansion coefficient for a perovskite ceramic and is usually in the range of 8–10 ppm/°C [29,30], it would be justified to infer from the present investigation that the vitreous material possesses a negative τ_f value. Fig. 7(b) shows the influence of sintering temperature on τ_f value in the $x = 10$ and $x = 15$ samples. As the sintering temperature increases, there is little variation in τ_f value in the $x = 10$ sample, while the τ_f value varies significantly in the $x = 15$ sample. It first decreases as sintering temperature rises from 940 °C to 1020 °C when the sintering temperature reaches 1060 °C, possibly a result of the increase of $Ca_2Nb_2O_7$-type pyrochlore phase. Optimal microwave dielectric properties of $\varepsilon_r = 32.0$, $Q_f = 6.64$ THz and $\tau_f = -27.1$ ppm/°C can be obtained in 15 wt% ZBS glass doped CLNZ ceramic when sintered at 940 °C for 4 h. The thermal expansion coefficient of the sample is 15.3 ppm/°C in the temperature range from room temperature to 800 °C, as illustrated in Fig. 8, suggesting the ceramic is suitable for surface mounting on PCB substrate since its thermal expansion coefficient matches rather well with that of PCB substrate (12–20 ppm/°C) [31]. In addition, the thermal conductivity of the sample is 2.4 W/mK, which means the 15 wt% ZBS glass doped CLNZ ceramic has good heat dissipation capacity for the packaged LTCC.

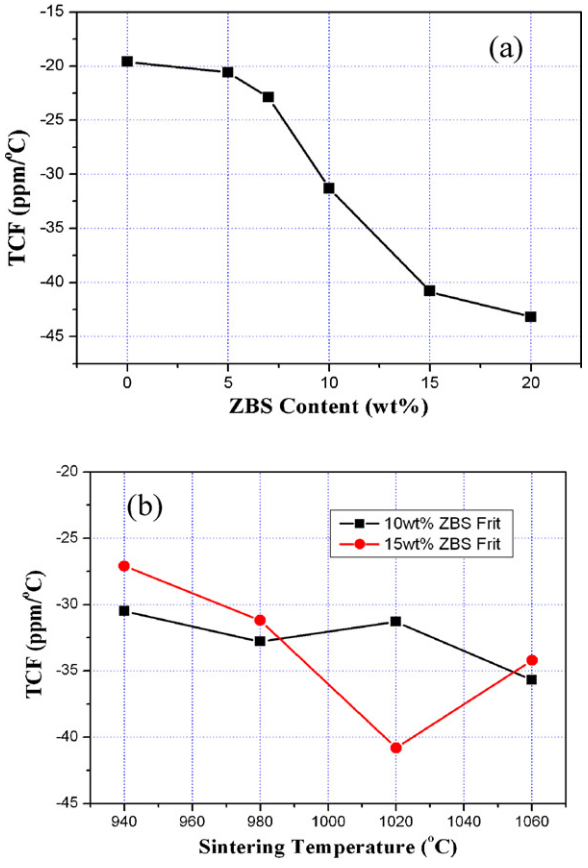

Fig. 7. τ_f varied with (a) ZBS glass doping content in CLNZ ceramics sintered at 1020 °C for 4 h and (b) variation of τ_f value with sintering temperatures in CLNZ + x wt% ZBS ceramics (where $x = 10$ and 15).

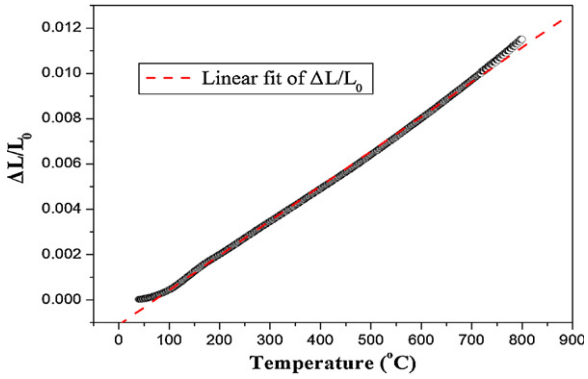

Fig. 8. Thermal expansion coefficient of 15 wt% ZBS doped CLNZ ceramic in the temperature range from room temperature to 800 °C.

For the investigation of cofiring property with Ag, about 20 wt% high purity conductive Ag slurry (Ag content > 80 wt%) was added to CLNZ + 15 wt% ZBS calcined powder, mixed manually using agate mortar and pestle. After drying, the powder was pelleted and sintered at 940 °C for 4 h. As illustrated in the XRD pattern in Fig. 9(a), the diffraction peaks of Ag cubic phase can be clearly indexed in terms of PCPDF card No. 87-0720. Besides CLNZ and Ag phase, no other diffraction peaks can be observed from the XRD pattern. It can also be seen from Fig. 9(b) and (c) that the Ag particles are embedded in the ceramic matrix with a highly visible grain boundary. Such evidence suggests the absence of chemical reaction between Ag and CLNZ ceramic or ZBS glass. Moreover, in order to check whether Ag metal migrates along grain boundaries and creates conduction pathways in the above ceramic, we tested the variation of the Q_f value in 15 wt% ZBS doped CLNZ ceramic before and after coating with Ag electrode. The Q_f value before coating with Ag electrode is 6.64 THz, while after the coating and scraping off excess Ag process, the Q_f value has become 6.29 THz. The variation is only within 5.3%, showing the conductive loss of the sample is hardly modified by Ag cofiring. Thus, 15 wt% ZBS glass doped CLNZ ceramic could be a potential LTCC material for applications in electronic industry providing that the τ_f value can be further modified.

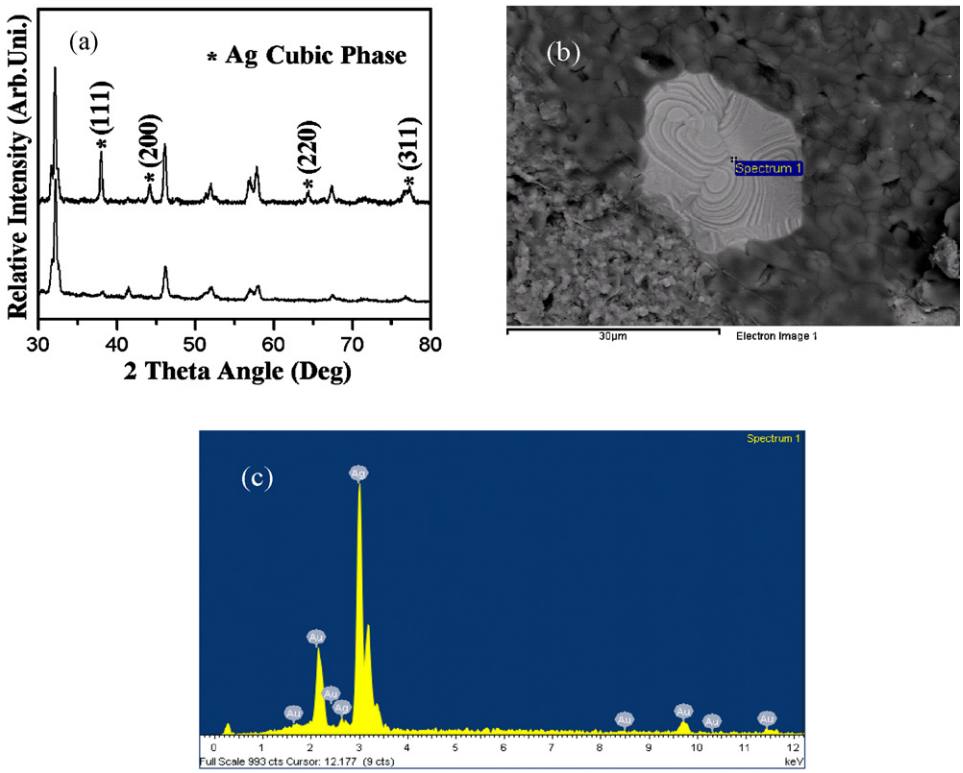

Fig. 9. Cofiring experiment of Ag with 15 wt% ZBS doped CLNZ ceramics sintered at 940 °C for 4 h. (a) XRD patterns, (b) SEM photograph and (c) EDS spectrum of the white particle.

4. Conclusion

Sintering behaviors and microwave dielectric properties of $Ca[(Li_{1/3}Nb_{2/3})_{0.95}Zr_{0.15}]O_{3+\delta}$ ceramic doped with ZBS frit have been investigated. The XRD patterns illustrate that a single perovskite phase can be obtained in ZBS doped CLNZ ceramics when the doping content is lower than 10 wt%. However, minor $Ca_2Nb_2O_7$-type pyrochlore phase appears when ZBS doping content reaches 15 wt% and its relative content increases with increasing ZBS doping content as well as sintering temperature. The (1 0 1) crystal plane in CLNZ perovskite has become preferred orientation with increasing ZBS content and sintering temperature, indicating that the (1 0 1) crystal plane possesses higher growth energy than that of the (1 2 1) crystal plane and that it prefers to grow under the inducement of ZBS vitreous phase or at higher sintering temperature. The ZBS vitreous phase segregates at grain boundary in the final ceramics, helping the densification process of CLNZ ceramic as well as lowering the sintering temperature by over 200 °C. Both the dielectric constant and Q_f value change similarly with the relative density in low ZBS doping content range of 5–10 wt%, but later the $Ca_2Nb_2O_7$-type impurity phase begins to positively contribute to both the ε_r and Q_f values and causes the variation trend to deviate from the relative density. The τ_f value has become more negative as the ZBS doping content increases. The optimal microwave dielectric properties of $\varepsilon_r = 32.0$, $Q_f = 6.64$ THz and $\tau_f = -27.1$ ppm/°C can be obtained in 15 wt% ZBS doped CLNZ ceramic when sintered at 940 °C for 4 h. The thermal expansion coefficient and the thermal conductivity of the ceramic are 15.3 ppm/°C and 2.4 W/mK respectively, suggesting it is suitable for surface mounting on PCB substrate. The cofiring experiment with Ag metal clearly shows that the ZBS doped CLNZ ceramic is both chemically and electrically compatible with Ag and has potential applications in LTCC industry if the τ_f value can be further adjusted to nearly zero.

Acknowledgments

This work was supported by the Hong Kong Innovation and Technology Fund (ITP 026/09NP). Hu, Xiong, Gu and Chen also thank the support from the National Science Foundation of China (No. 61076049), the Industry-University-Research Institute Foundation of Guangdong Province (2009B090300368) and the Natural Science Foundation of Guangdong Province (Grant No. 9151063101000040).

References

[1] Y.-X. Guo, Z.-Y. Zhang, L.-C. Ong, M.-Y.-W. Chia, A novel LTCC miniaturized dualband balun, IEEE Microwave Wireless Components Letters 16 (2006) 143–145.
[2] A. Ariffin, S. Bujang, M.-F. Amiruddin, S. Jaafar, N.-A.-M. Akib, Y.-C. Lee, LTCC SoP RF transceiver module for 60 GHz wireless gigabit Ethernet communication system, Journal of Communication and Computer 7 (2010) 63–70.
[3] E. Mis, A. Dziedzic, K. Nitsch, Electrical properties and electrical equivalent models of thick-film and LTCC microcapacitors, Microelectronic International 26 (2009) 45–50.

[4] J. Laskar, S. Pinel, C.H. Lee, S. Sarkar, B. Perumana, J. Papapolymerou, E. Tentzeris, Circuit and module challenges for 60 GHz Gb/s radio, IEEE/ACES International Conference on Wireless Communication and Applied Computer Electromagnetic 15 (2005) 447–450.
[5] J.-W. Choi, C.-Y. Kang, S.-J. Yoon, H.-J. Kim, H.-J. Jung, K.-H. Yoon, Microwave dielectric properties of $Ca[(Li_{1/3}Nb_{2/3})_{1-x}M_x]O_{3-\delta}$ (M = Sn, Ti) ceramics, Journal of Material Research 14 (1999) 3567–3570.
[6] D.-W. Kim, K.-H. Ko, K.-S. Hong, Influence of copper(II) oxide additions to zinc niobate microwave ceramics on sintering temperature and dielectric properties, Journal of American Ceramic Society 84 (2001) 1286–1290.
[7] S. George, P.-S. Anjana, V.-N. Deepu, P. Mohanan, M.-T. Sebastian, Low temperature sintering and microwave dielectric properties of Li_2MgSiO_4 ceramics, Journal of American Ceramic Society 92 (2009) 1244–1249.
[8] M.-Z. Jhou, J.-H. Jean, Low-fire processing of microwave $BaTi_4O_9$ dielectric with $BaO–ZnO–B_2O_3$ glass, Journal of American Ceramic Society 89 (2006) 786–791.
[9] P. Liu, E.-S. Kim, K.-H. Yoon, Low-temperature sintering and microwave dielectric properties of $Ca(Li_{1/3}Nb_{2/3})O_{3-\delta}$ ceramics, Japanese Journal of Applied Physics 40 (2001) 5769–5773.
[10] J.-W. Choi, C.-Y. Kang, S.-J. Yoon, Microwave dielectric properties of B_2O_3 doped $Ca[(Li_{1/3}Nb_{2/3})_{0.9}Ti_{0.1}]O_{3-\delta}$ ceramics, Ferroelectrics 262 (2001) 167–172.
[11] H. Jantunen, R. Rautioaho, A. Uusimäki, S. Leppävuori, Compositions of $MgTiO_3–CaTiO_3$ ceramic with two borosilicate glasses for LTCC technology, Journal of European Ceramic Society 20 (2000) 2331–2336.
[12] H.-K. Zhu, M. Liu, H.-Q. Zhou, L.-Q. Li, A.-G. Lv, Study on properties of $CaO–B_2O_3–SiO_2$ system glass–ceramic, Material Research Bulletin 42 (2007) 1137–1144.
[13] S. Thomas, M.-T. Sebastian, Effect of $B_2O_3–Bi_2O_3–SiO_2–ZnO$ glass on the sintering and microwave dielectric properties of $0.83ZnAl_2O_4–0.17TiO_2$, Material Research Bulletin 43 (2008) 843–851.
[14] A.R. von Hippel, Dielectric Materials and Applications, The MIT Press, Cambridge, MA, 1954.
[15] T. Takada, S.-F. Wang, S. Yoshikawa, S.-J. Jang, R.-E. Newnham, Effect of glass additions on $BaO–TiO_2–WO_3$ microwave ceramics, Journal of American Ceramic Society 77 (1994) 1909–1916.
[16] R.M. Germen, Liquid Phase Sintering, Plenum Publishing, New York, 1985, p. 239.
[17] L.-C. Chang, B.-S. Chiou, Effect of B_2O_3 nano-coating on the sintering behaviors and electrical microwave properties of $Ba(Nd_{2-x}Sm_x)Ti_4O_{12}$ ceramics, Journal of Electroceramic 13 (2004) 829–837.
[18] K.-H. Lin, C.-L. Liao, S.-T. Lin, A study on the interfacial reaction and dielectric properties of $Ba_{0.88}(Nd_{1.40}Bi_{0.42}La_{0.30})Ti_4O_{12}$ alkali-borosilicate glass composites, Ceramic International 36 (2010) 2365–2374.
[19] Y.-C. Lee, S.-Y. Park, M.-K. Choi, S.-O. Yoon, Effect of grain orientation on abnormal grain growth in Ba-hexaferrite, Ceramic International 27 (2001) 215–218.
[20] M.-Z. Hu, J. Qian, H.-S. Gu, Y.-D. Hao, Phase formation, sintering behavior and microwave dielectric properties of bismuth and manganese co-doped $[(Pb,Ca)La](Fe,Nb)O_{3+\delta}$ solid solution, Journal of Material Science 41 (2006) 6260–6265.
[21] S.-H. Yoon, D.-W. Kim, S.-Y. Cho, K.-S. Hong, Investigation of the relations between structure and microwave dielectric properties of divalent metal tungstate compounds, Journal of European Ceramic Society 26 (2006) 2051–2054.
[22] Y.-C. Chen, P.-S. Cheng, C.-F. Yang, W.-C. Tzou, Substitution of CaO by BaO to improve the microwave dielectric properties of $CaO–Li_2O–Sm_2O_3–TiO_2$ ceramics, Ceramic International 27 (2001) 809–813.
[23] M.-Z. Hu, H.-S. Gu, X.-C. Chu, J. Qian, Z.-G. Xia, Crystal structure and dielectric properties of $(1-x)Ca_{0.61}Nd_{0.26}TiO_3 + xNd(Mg_{1/2}Ti_{1/2})O_3$ complex perovskite at microwave frequencies, Journal of Applied Physics 104 (2008) 124104.
[24] R.-J. Cava, J.-J. Krajewski, R.-S. Roth, Low temperature coefficient bulk dielectrics in the $Ca_2Nb_2O_7–Ca_2Ta_2O_7$ system, Material Research Bulletin 33 (1999) 527–532.
[25] K.-P. Surendran, P. Mohanan, M.-T. Sebastian, The effect of glass additives on the microwave dielectric properties of $Ba(Mg_{1/3}Ta_{2/3})O_3$ ceramics, Journal of Solid State Chemistry 177 (2004) 4031–4046.
[26] Q. Zeng, W. Li, J.-L. Shi, X.-L. Dong, J.-K. Guo, Influence of V_2O_5 additions to $5Li_2O–1Nb_2O_5–5TiO_2$ ceramics on sintering temperature and microwave dielectric properties, Journal of American Ceramic Society 90 (2007) 2262–2265.
[27] E.-L. Bourhis, Glass: Mechanics and Technology, Wiley-VCH Publishing, 2007,, p. 54.
[28] T. Joseph, M.-T. Sebastian, H. Sreemoolanadhan, V.K.-S. Nageswari, Effect of glass addition on the microwave dielectric properties of $CaMgSi_2O_6$ ceramics, International Journal of Ceramic Technology 7 (2010) E98–E106.
[29] I.-M. Reaney, E.-L. Colla, N. Setter, Dielectric and structural characteristics of Ba- and Sr-based complex perovskites as a function of tolerance factor, Japanese Journal of Applied Physics 33 (1994) 3984–3990.
[30] E.-L. Colla, I.-M. Reaney, N. Setter, Effect of structural changes in complex perovskites on the temperature coefficient of the relative permittivity, Journal of Applied Physics 74 (1993) 3414–3425.
[31] V. Gektin, A. Barcohen, S. Witzman, Coffin-Manson based fatigue analysis of underfilled DCAS, IEEE Transactions on Components, Packaging and Manufacturing Technology, Part A 21 (1998) 577–584.